Available online at www.sciencedirect.com

ScienceDirect

Energy Procedia 76 (2015) 463 – 469

Energy Procedia

European Geosciences Union General Assembly 2015, EGU

Division Energy, Resources & Environment, ERE

Seismic attribute analysis of the indicator for gas hydrate occurrence in the northwest Ulleung Basin, East Sea

Kyoung Jin Kim[a], Bo Yeon Yi[b], Nyeon Keon Kang[b], Dong Geun Yoo[b*]

[a]*Korea University of Science and Technology (UST), 217 Gajeong-ro, Yuseong-gu, Daejeon, 305-350*

[b]*Korea Institute of Geoscience and Mineral Resources (KIGAM),124 Gwahang-no, Yuseong-gu, Daejeon, 305-350, Korea*

Abstract

Based on the interpretation of 3D seismic profiles, the shallow sediments consist of five seismic units. BSRs and acoustic blanking are located within the gas-hydrate stability zone as indicators for the presence of gas hydrate. Seismic-attribute analysis shows that if gas hydrates are underlain by free gas, high reflection strength and low instantaneous frequency are displayed below the BSR. Whereas, if not, reflection strength is low and instantaneous frequency is continuously high. Four models for the occurrence of the gas hydrate are suggested, considering the slope of sedimentary layers as well as the presence of gas hydrate or free gas.

Peer-review under responsibility of the GFZ German Research Centre for Geosciences

Keywords: *Ulleung Basin, gas hydrate, seismic attribute analysis, BSR (bottom simulating reflector), acoustic blanking, UBGH2 (the Second Ulleung Basin Gas Hydrate Drilling Expedition)*

1. Introduction

Gas hydrates are an ice-like compound of natural gas (mainly methane) and water formed under low-temperature and high-pressure conditions. Because gas hydrates contain methane and occur in deep-water or permafrost regions all over the world, they have potential as alternative energy resources for the future [1]. In addition, gas hydrates

* Corresponding author. Tel.: +82-42-868-3324; Fax: +82-42-868-3417
E-mail address: dgyoo@kigam.re.kr

Peer-review under responsibility of the GFZ German Research Centre for Geosciences
doi:10.1016/j.egypro.2015.07.882

play potentially important roles in greenhouse effect and in underwater slope failure if they are warmed or distributed enough that the gas is dissociated from the ice. In the case of Korea, gas hydrate research was initiated by the Korea Institute of Geoscience and Mineral Resources (KIGAM) in 1996 [2]. Significant amounts of geophysical survey data containing 2D and 3D seismic data, as well as core data were acquired, and two Ulleung Basin Gas Hydrate Drilling Expeditions (UBGH) were performed (2007 and 2010).

The presence of gas hydrate can be determined using bottom simulating reflectors (BSRs), acoustic blanking, seismic chimneys, and enhanced reflectors in the seismic sections. In the northwest Ulleung Basin, it was reported that BSRs and acoustic blanking were identified as indicators of gas-hydrate occurrence within turbidites or hemipelagic sediments [3]. The BSR has high reflection amplitude because it is at the boundary between upper gas hydrate and lower free gas, and generates a high acoustic-impedance contrast. Acoustic blanking is defined as the reduction in amplitude of reflectors caused by the cementation effect of gas hydrate within sediment pore spaces.

Seismic attribute analysis including reflection strength, instantaneous frequency, and spectral decomposition can be used for a geophysical indicator representing the presence of gas hydrate or free gas [4]. However, in the case of Korea, although a significant amount of seismic data has been acquired, there has been grossly inadequate study using seismic attribute analysis to investigate the occurrence of gas hydrate.

In this paper, we reveal the sedimentary and structural development aspects of the sedimentary sequence, including the gas hydrate stability zone (GHSZ), through seismic unit analysis. From seismic attribute analysis, we describe the characteristics indicating the occurrence of gas hydrate and free gas.

2. Study area and data set

The East Sea is a semi-enclosed marginal sea bounded by the coast of northeastern Asia and the islands of Japan. The sea is now connected by narrow straits to the Western Pacific, East China Sea, and Okhotsk Sea (Fig. 1A).

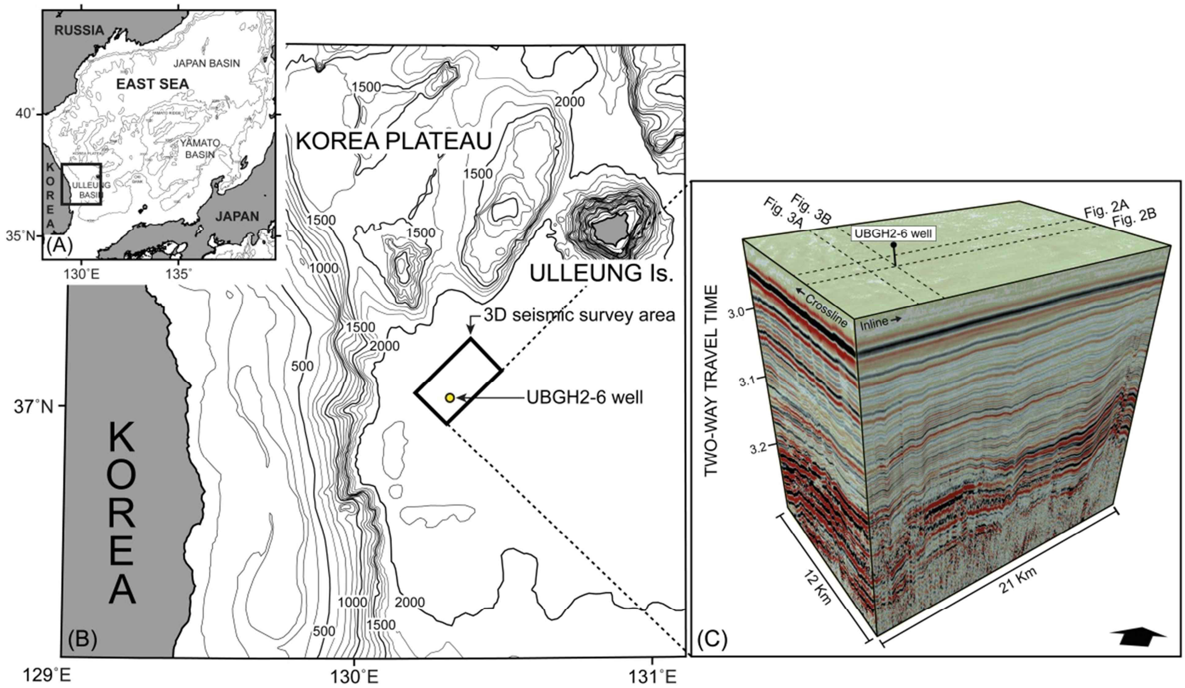

Fig. 1. (A) Physiography of the East Sea (contour interval is 1 km). (B) Bathymetry map of the northwestern area of the Ulleung Basin. (C) 3D seismic cube and drilling site UBGH2-6.

The Ulleung Basin is a bowl-shaped back-arc basin located in the southwestern East Sea (Figs. 1A and 1B). The basin gradually deepens northeastward and the basin floor lies at water depths of 2000-2300 m. The Basin is bounded by the Korea Plateau to the north, and eastern Korea Peninsula to the west, with a steep gradient of up to 10°. The southern and eastern margins are bounded by the Japan Islands and the Oki Bank, with a relatively gentle slope, less than 3°.

The study area in the northwest Ulleung Basin is a deep basin floor far from the Korea Plateau and from the steep slope of the eastern Korean Peninsula. The sedimentary sequence including the GHSZ, is dominated by turbidites and hemipelazites deposited under low-energy conditions.

The data used in this study consist of 3D seismic data and well-log data from the drilling site UBGH2-6 (Fig. 1B). The total area of the 3D seismic survey is about 200 km^2 (21 km × 12 km) (Fig. 1C). The acquired data was processed using Prestack Kirchhoff time migration by Western Geco. The recording length is 5.5 s, and sampling interval is 1ms. The drilling site UBGH2-6 is located within the 3D seismic survey area in the north-most part of the Ulleung Basin. Logging while drilling (LWD), wire-line logging (WL), and vertical seismic profiling (VSP) were performed. In this study, resistivity and velocity logs were used to identify the occurrence of gas hydrate.

3. Seismic unit analysis

Based on the interpretation of the seismic data, the shallow sedimentary sequence including the GHSZ, consists of five seismic units (Unit 1 to Unit 5 in Figs. 2 and 3) separated by five key reflectors (H1 to H5 in Figs. 2 and 3). Units 1 to 4 show low amplitude because they are dominated by homogeneous hemipelagic muds, but Unit 5 is characterized by high amplitude due to the hemipelagic muds intercalated with turbidite sands. The reflectors are generally parallel except for mass transport deposits (MTDs) showing chaotic reflectors. It was reported that the frequency of turbidite sediments increases, and the maximum thickness of the sandy bed is over 50 cm, in Unit 5 [5].

A gentle anticline is present in the study area that documents the activity of many faults. The curvature of the anticline gradually increases from H1 to H5 and the sedimentary strata incline downward on the limb of the anticline, especially toward the southwest (Fig. 2).

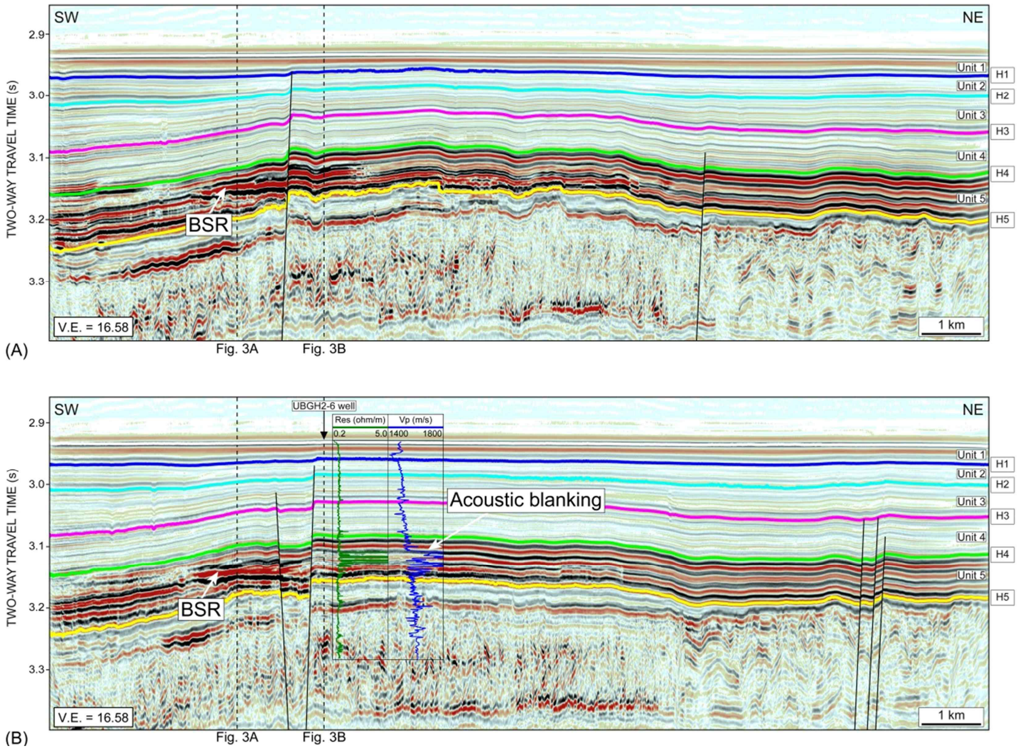

Fig. 2. Seismic profiles of (A) Inline 1237 and (B) Inline 1292 (for location, see Fig. 1C). Green and blue lines indicate the resistivity and velocity logs respectively. Vertical black lines indicate the faults.

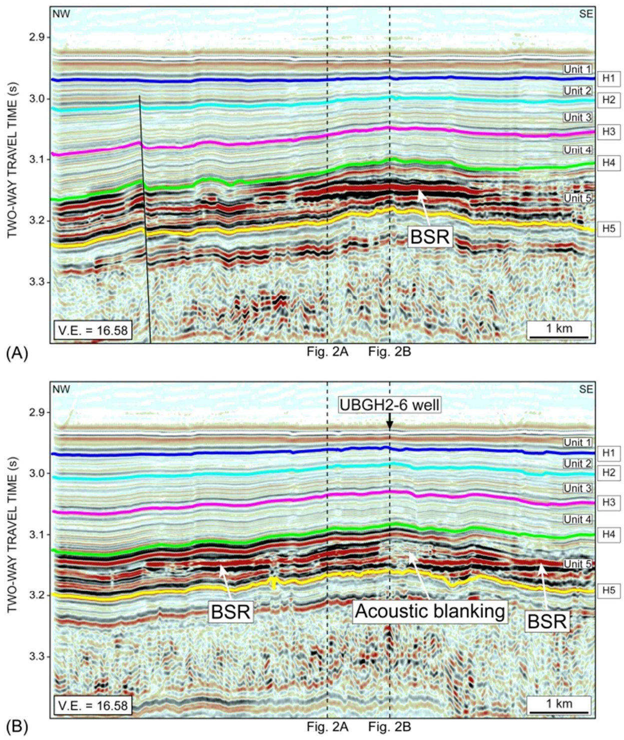

Fig. 3. Seismic profiles of (A) Crossline 1818 and (B) Crossline 2124 (for location, see Fig. 1C).

Acoustic blanking and BRS in Unit 5 indicate the presence of gas hydrate (Figs. 2 and 3). The BSR runs almost parallel to the seafloor and cross-cuts the dipping reflectors on the limb of the anticline. It also has high amplitude and reversed polarity with respect to the seafloor. The acoustic blanking zone in the logs has high velocity and resistivity in the gas hydrate occurrence zone (GHOZ) (Fig. 2B). It shows low amplitude and is mainly located on the crest of the anticline. Especially, large-scaled two faults are located near the seismic indicators including the BSR and acoustic blanking (Fig. 2B). They dip southwestward and are defined as high-angle faults with apparent dip over 51°.

4. Seismic attribute analysis

The arbitrary seismic profile including the BSR and acoustic blanking was used for the analysis of reflection strength and instantaneous frequency. And, a spectral decomposition was performed in steps from 10 to 70 Hz to identify whether the free gas is preserved below the BSR.

4.1. Reflection strength

High reflection strength is indicated at the BSR on the southwest limb of the anticline (HRS-1 in Fig. 4A), and also displayed upon the BSR (HRS-2 in Fig. 4A). On the crest of the anticline, the acoustic blanking zone with low reflection strength is identified which is equal to the GHOZ because it has high resistivity and velocity logs (LRS in Fig. 4A). At the specific area below the acoustic blanking zone, reflection strength is high (HRS-3 in Fig. 4A). A small high reflection strength interval is identified in the MTDs located below 3.2 s.

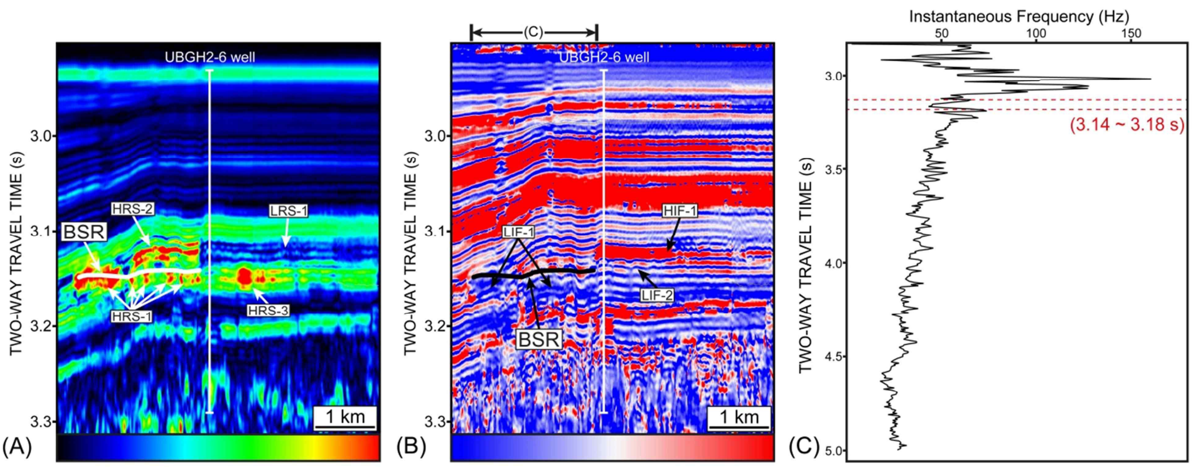

Fig. 4. The results of seismic attribute analysis including (A) Reflection strength and (B) Instantaneous frequency; (C) Vertical distribution chart of instantaneous frequency (for location, see Fig. 4B); HRS: high reflection strength, HIF: high instantaneous frequency, LRS: low reflection strength, LIF: low instantaneous frequency.

4.2. Instantaneous frequency

Instantaneous frequency decreases sharply below the BSR (LIF-1 in Fig. 4B). Based on the vertical distribution chart of instantaneous frequency, it clearly decreases from 120 Hz to 40 Hz below the BSR; however, a little low instantaneous frequency appears above the BSR. The GHOZ shows high instantaneous frequency (over 90) where the reflection strength is very low (HIF in Fig. 4B). Below the GHOZ, instantaneous frequency decreases, but it is less than below the BSR (LIF-2 in Fig. 4B).

4.3. Spectral decomposition

Based on the result of spectral decomposition, a very high envelope (over 4000) is displayed at the BSR in the 50 Hz frequency domain. It decreases sharply at greater than 50 Hz.

5. Gas hydrate and free gas

Four models for the occurrence of gas hydrate and free gas are suggested considering the slope of sedimentary layers as well as the presence of seismic indicators for the presence of gas hydrate: (1) dipping strata with strong BSR, (2) parallel strata with acoustic blanking and weak BSR, (3) parallel strata with acoustic blanking, and (4) dipping strata with no seismic indicators (Fig. 5).

In Model 1, the gas hydrate overlying free gas zone within dipping strata generates strong BSR due to acoustic impedance contrast (Fig. 5B; Table 1). In addition, the tuning effect which is generated between the BSR and the lower boundary of the free gas zone increases the amplitude of the BSR. Following the spectral decomposition of the BSR, a high envelope (over 4000) is displayed at 50 Hz. It was reported that a high envelope anomaly at this specific high frequency range indicates generation of the tuning effect due to the lower free gas content [6]. Reflection strength is high at the BSR due to the acoustic-impedance contrast between gas hydrate and free gas. Instantaneous frequency decreases sharply below the BSR because free gas bearing sediments generate the attenuation of high frequency components [7]. In Model 2, the gas hydrate overlying the free gas zone is located within parallel strata (Fig. 5C; Table 1). Although, the BSR is developed by acoustic-impedance contrast between gas hydrate and free gas, the amplitude is low due to the absence of the tuning effect within parallel strata. In Model 3, the gas hydrate occurs within parallel strata without free gas (Fig. 5D; Table 1). Below the GHOZ, the resistivity log reduces to background value, but the high velocity log persists and is continuous. It indicates the presence of water-bearing sand below the GHOZ without free gas [5]. Therefore, the BSR is not generated because the acoustic-impedance contrast is so low between the gas hydrate bearing and water bearing formations. Instantaneous frequency is continually high below the GHOZ. Last, in Model 4, no seismic indicators are developed because of the absence of gas hydrate and free gas (Fig. 5E; Table 1).

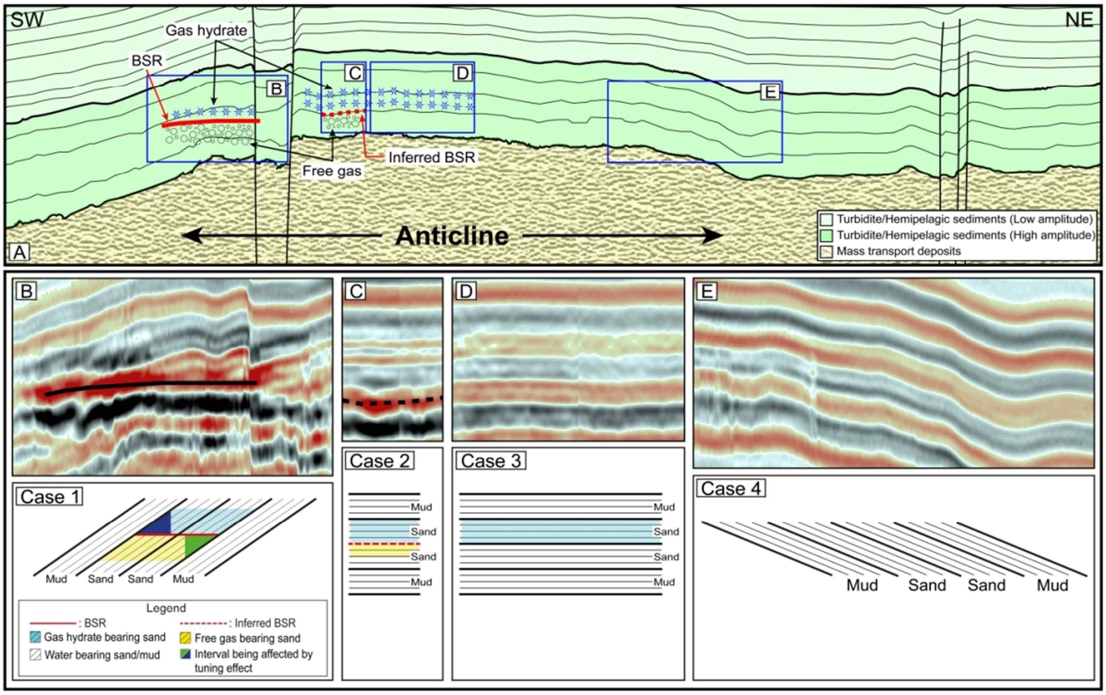

Fig. 5. (A) A schematic diagram showing (B) to (E) the four models for the occurrence of gas hydrate and free gas.

Table 1. Results of seismic attribute analysis for the four models and their interpretation.

Case	Seismic characteristics	Seismic attribute			Seismic appearance [3]	Interpretation
		Reflection strength [1]	Instantaneous frequency [2]	Seismic appearance [1]		
1	Strong BSR within dipping strata	High	From high to very low	High envelope at specific high frequency range	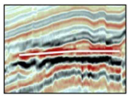	Strong BSR is generated by acoustic impedance contrast between hydrate and free gas, and tuning effect enhances the amplitude of BSR
2	Weak BSR within parallel strata Acoustic blanking interval upon the BGHSZ [4]	High	From very high to low	-	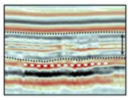	BSR is generated by acoustic impedance constrast between hydrate and free gas , but the amplitude of BSR is so low due to the absence of the tuning effect
3	Parallel strata without BSR Acoustic blanking interval upon the BGHSZ	Low	From very high to high	-	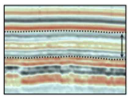	BSR is not generated because the acoustic impedance contrast between hydrate and water-bearing sand is so low. This is equal to the result of core analysis showing the none of free gas beneath the GHOZ from UBGH2-6 well
4	Dipping strata without BSR	Low	-	-	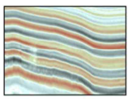	BSR is not generated due to the absence of hydrateand free gas

[1] Reflection strength and spectral decomposition results at the BGHSZ(base of gas hydrate stability zone)
[2] The change of instantaneous frequency downward across the BGHSZ
[3] Each white bold and dotted line indicates the strong and weak BSR(bottom simulating reflector) respectively, and the acoustic blanking interval between black dotted lines is the GHOZ (gas hydrate occurrence zone) identified by the analysis of cores acquired from UBGH2-6 well
[4] The depth of BGHSZ is similar to the depth of BSR

6. Conclusions

Based on the interpretation of 3D seismic data, the shallow sedimentary sequence including the GHSZ consists of five seismic units separated by regional reflectors. The anticline that is present in the study area plays an important role in the slope of the layers. The seismic indicators for the occurrence of gas hydrate, including the BSR and acoustic blanking coincident with high resistivity and velocity logs, are located in the GHSZ. Seismic-attribute analysis shows that if gas hydrate overlying free gas occurs, the reflection strength is high and instantaneous frequency decreases sharply below the gas hydrate zone. Whereas, if gas hydrate occurs without free gas, reflection strength is low and instantaneous frequency is high continuously below the gas hydrate zone. A model for the occurrence of gas hydrate and free gas can be suggested based on the presence of seismic indicators and on the gradient of the sedimentary strata.

Acknowledgements

This study is a contribution by the gas hydrate R&D project of Ministry of Trade, Industry and Energy, Korea. We also thank the Gas Hydrate R/D Organization (GHDO) for funding.

References

[1] Kvenvolden KA. Gas hydrate-geological prospective and global change. Reviews of Geophysics 1993; 31: 173-187.
[2] Ryu BJ, Collett TS, Riedel M, Kim GY, Chun JH, Bahk JJ, Lee JY, Kim JH, Yoo DG. Scientific results of the Second Gas Hydrate Drilling Expedition in the Ulleung Basin (UBGH2). Marine and Petroleum Geology 2013; 47: 1-20.
[3] Yoo DG, Kang NK, Yi BY, Kim GY, Ryu BJ, Lee KS, Lee GH, Riedel M. Occurrence and seismic characteristics of gas hydrate in the Ulleung Basin, East Sea. Marine and Petroleum Geology 2013; 47: 236-247.
[4] Thakur NK, Rajput S. Exploration of Gas hydrates: Geophysical Techniques. Springer, Berlin: 2011.
[5] Bahk JJ, Kim GY, Chun JH, Lee JY, Ryu BJ, Lee JH, Son BK, Collett TS. Characterization of gas hydrate reservoirs by integration of core and log data in the Ulleung Basin, East Sea. Marine and Petroleum Geology 2013; 47: 30-42.
[6] Oliveira S, Vilhena O, Casta E. Time-frequency spectral signature of Pelotas Basin deep water gas hydrate system. Marine Geophysical Research 2010; 31: 89-97.
[7] Taylor MH, Dillon WP, Pecher IA. Trapping and migration of methane associated with the gas hydrate stability zone at the Blake Ridge Diapir: new insights from seismic data. Marine Geology 2000; 164: 79-89.